

The magnetization process in the 2-dimensional $J_1 - J_2$ model

A. Fledderjohann, K.-H. Mütter

Physics Department, University of Wuppertal, 42097 Wuppertal, Germany

We study the $\alpha = J_2/J_1$ -dependence of the magnetization process in the $J_1 - J_2$ model on a square lattice with frustrating couplings J_2 along the diagonals. Perturbation expansions around $\alpha = J_2/J_1 = 0$ and $\alpha^{-1} = 0$ yield an adequate description of the magnetization curve in the antiferromagnetic and collinear antiferromagnetic phase, respectively. The transition from one phase to the other ($0.5 < \alpha < 0.7$) leaves pronounced structures in the longitudinal and transverse structure factors at $\mathbf{p} = (\pi, \pi)$ and $\mathbf{p} = (0, \pi)$.

75.10.-b, 75.10.Jm

I. INTRODUCTION

Magnetization processes in quasi one-dimensional quantum spin systems have been studied intensively during the last years. The Oshikawa, Yamanaka and Affleck quantization rule¹ predicts possible plateaus in the magnetization curve at certain rational values of the magnetization M , which can be derived either from the geometry of the unit cell or a mapping onto a one-dimensional system with modulated couplings.²

In the latter formulation, the plateaus appear at those values where the wave vector of the modulation coincides with the soft mode momenta of the unperturbed system. The existence of soft modes (zero energy excitations) is guaranteed by the Lieb Schultz Mattis theorem³ for translation invariant, one-dimensional systems with finite-range couplings. A rigorous extension of this important theorem to two and three-dimensional systems does not exist to date. For this reason, the Oshikawa, Yamanaka and Affleck quantization rule cannot be applied in a straightforward way to predict possible plateaus in the magnetization curves of two- and three-dimensional systems.

Experimental results, however, just concern compounds with a higher dimensional coupling structure as there are:

(A) $CsCuCl_3$ [Ref. 4] Here, a plateau has been found at $M/M_s = 1/3$ ($M_s = 1/2$ is the saturating magnetization). An explanation of this feature has been given in Ref. 5.

(B) NH_4CuCl_3 [Ref. 6] Here, magnetization plateaus have been found for $M/M_s = 1/4, 3/4$. The compound is suggested to be built up as a two-dimensional structure of interacting two leg zig-zag ladders.⁷

(C) $SrCu_2(BO_3)_2$ [Ref. 8] Magnetization plateaus have been observed for $M/M_s = 1/3, 1/4, 1/8$. The compound is modelled by the two-dimensional Shastry Sutherland model.⁹⁻¹¹ An explanation of the plateaus at $M/M_s = 1/4, 1/3$ has been discussed in Ref. 12.

In this paper we are going to study the magnetization process in a two-dimensional spin-1/2 Heisenberg model with Hamiltonian

$$H = J_1 H_1 + J_2 H_2 - B S_3(\mathbf{p} = \mathbf{0}) \quad (1.1)$$

with isotropic couplings

$$H_l = \sum_{\mathbf{x}, \mathbf{y}} J_l(\mathbf{x}, \mathbf{y}) \mathbf{S}(\mathbf{x}) \cdot \mathbf{S}(\mathbf{y}), \quad l = 1, 2 \quad (1.2)$$

for nearest and next-to-nearest neighbour sites x and y :

$$J_1(\mathbf{x}, \mathbf{y}) = \delta_{\mathbf{y}, \mathbf{x} + \hat{1}} + \delta_{\mathbf{y}, \mathbf{x} + \hat{2}} \quad (1.3)$$

$$J_2(\mathbf{x}, \mathbf{y}) = \delta_{\mathbf{y}, \mathbf{x} + \hat{1} + \hat{2}} + \delta_{\mathbf{y}, \mathbf{x} + \hat{1} - \hat{2}}; \quad (1.4)$$

$\hat{1}$ and $\hat{2}$ denote lattice vectors in horizontal and vertical directions. For convenience we choose the nearest neighbour coupling to be one ($J_1 = 1$, i.e. $\alpha = J_2/J_1 = J_2$) and use

$$S_j(\mathbf{p}) = \sum_{\mathbf{x}} e^{i\mathbf{p} \cdot \mathbf{x}} S_j(\mathbf{x}), \quad j = 1, 2, 3 \quad (1.5)$$

for the Fourier transform of the spin operators on the square lattice.

If we assume periodic boundary conditions the Hamiltonian (1.1) is translationally invariant. Moreover it commutes with the total spin operators $\mathbf{S}^2(\mathbf{p} = \mathbf{0})$ and $S_3(\mathbf{p} = \mathbf{0})$. We will classify the eigenstates $|E, \mathbf{p}, s, s_3\rangle$ by the eigenvalues:

$$\begin{array}{ll} E & \text{of } H_1 + \alpha H_2, \\ \mathbf{p} = (p_1, p_2) & \text{of the momentum operator,} \\ s(s+1) & \text{of the squared total spin } \mathbf{S}^2(\mathbf{p} = \mathbf{0}), \\ s_3 & \text{of the 3-component } S_3(\mathbf{p} = \mathbf{0}). \end{array}$$

The magnetization curve $M = M(B)$ is computed from the energy differences

$$B(M = s/N, \alpha) = E(s+1, \mathbf{p}_{s+1}, \alpha) - E(s, \mathbf{p}_s, \alpha). \quad (1.6)$$

$E(s, \mathbf{p}_s, \alpha)$ is the lowest eigenvalue of $H_1 + \alpha H_2$ in the sector with total spin s . N is the total number of sites and \mathbf{p}_s is the ground state momentum in this sector.

\mathbf{p}_s can be deduced from Marshall's sign rule¹³ in the limiting cases $\alpha = 0$ and $\alpha \rightarrow \infty$.

a) $\alpha = 0$

$$\mathbf{p}_s = (0, 0) \quad \text{if } \frac{N}{2} + s \quad \text{is even} \quad (1.7)$$

$$\mathbf{p}_s = (\pi, \pi) \quad \text{if } \frac{N}{2} + s \quad \text{is odd,} \quad (1.8)$$

where the latter equations hold for clusters with size $N = L \times L$, L even and periodic boundary conditions. Therefore, the transition between two subsequent ground states as they enter on the left- and right-hand side of (1.6) is accompanied by a momentum transfer

$$\mathbf{q} = \mathbf{p}_{s+1} - \mathbf{p}_s = (\pi, \pi) \quad (1.9)$$

b) $\alpha \rightarrow \infty$

The Hamiltonian

$$H_2 = H_1^{(+)} + H_1^{(-)} \quad (1.10)$$

decays into two *nearest-neighbour* Hamiltonians on the even and odd sublattices, respectively. The nearest-neighbour couplings are defined here along the diagonals $\hat{1} + \hat{2}$, $\hat{1} - \hat{2}$. Seen from the original lattice, the diagonals are rotated by $\pm \frac{\pi}{4}$. Moreover, the lattice constant increases by a factor $\sqrt{2}$.

We conclude from this that the momentum transfer between the two subsequent ground states in (1.6) is here

$$\mathbf{q} = \mathbf{p}_{s+1} - \mathbf{p}_s = (\pi, 0), (0, \pi). \quad (1.11)$$

The change from (1.9) to (1.11) signals a phase transition from antiferromagnetic to collinear antiferromagnetic order.¹⁴

Linear spin wave theory predicts that the regimes for antiferromagnetic and collinear antiferromagnetic order are restricted to $\alpha < 0.4$ and $\alpha > 0.55$, respectively. In between a phase with transverse disorder has been suggested.¹⁵

We pursue the following strategy to study the impact of frustration on ground state energies and magnetization curves: We derive perturbation expansions in α and α^{-1} , which are aimed to describe adequately the behaviour in the antiferromagnetic and collinear antiferromagnetic phase, respectively. Comparison with computations on finite clusters indicates that the perturbation results agree for $\alpha < 0.5$ and $\alpha > 0.7$, respectively. The regime in between which is not accessible by perturbation methods is of special interest. Here, we expect the emergence of plateaus in the magnetization curve.^{15,16}

The outline of the paper is as follows: In Sec. II and Appendices A and B we present the results for the ground state energies obtained from perturbation expansions around $\alpha = 0$ and $\beta = 1/\alpha = 0$.

Free energies and magnetization curves are discussed in Sec. III. Numerical results on the lowest frequency moments of the dynamical structure factor for momenta $\mathbf{q} = (\pi, \pi)$ and $\mathbf{q} = (\pi, 0), (0, \pi)$ are given in Sec. IV.

II. FROM ANTIFERROMAGNETIC TO COLLINEAR ANTIFERROMAGNETIC ORDER

In the antiferromagnetic phase $\alpha < \alpha_0(M)$ perturbation theory up to second order yields for the lowest

eigenvalue of $H_1 + \alpha H_2$ in the sector with magnetization $M = s/N$:

$$E(s, \mathbf{p}_s, \alpha) = N (\epsilon_1(M) + \alpha \epsilon_2(M) + \alpha^2 \delta_2(M)) ; \quad \alpha < \alpha_0(M) \quad (2.1)$$

where

$$\epsilon_j(M) = \frac{1}{N} \langle 0 | H_j | 0 \rangle, \quad j = 1, 2 \quad (2.2)$$

are the expectation values of H_1 and H_2 determined for the unfrustrated ground states $|0\rangle$ (i.e. $H = H_1$).

The second order contribution $\delta_2(M)$ can be expressed in terms of the transition probabilities $|\langle n | H_2 | 0 \rangle|^2$ and energy differences $E_n - E_0$ between the ground state $|0\rangle$ and the excited states $|n\rangle$:

$$\delta_2(M) = -\frac{1}{N} \sum_n \frac{|\langle n | H_2 | 0 \rangle|^2}{E_n - E_0}. \quad (2.3)$$

The M -dependence of $\epsilon_1(M)$ and $\epsilon_2(M)$ is shown in Fig. 1(a) and 1(b) respectively for system sizes $N = 4 \times 4$ (with periodic boundary conditions) and $N = 5 \times 5 \mp 1 = 24, 26$ (with helical boundary conditions). The data points for $\epsilon_1(M)$ nicely scale in M ; deviations from scaling appear in $\epsilon_2(M)$ for smaller M values.

Numerical results for the second order contribution $\delta_2(M)$ obtained with the recursion method¹⁷ are shown in Fig. 2. Scaling in M is realized for larger M -values ($M > 0.3$). For $M = 0$ and $M = 1/4$, the $N = 4 \times 4 = 16$ data significantly deviate from the larger system results with $N = 5 \times 5 \mp 1$. We suggest that the deviations from scaling in $\epsilon_2(M)$ [Fig. 1(b)] and $\delta_2(M)$ [Fig. 2] arise from peculiarities of the 4×4 system¹⁸ and that the thermodynamical limit is fairly well approximated by the larger system results.

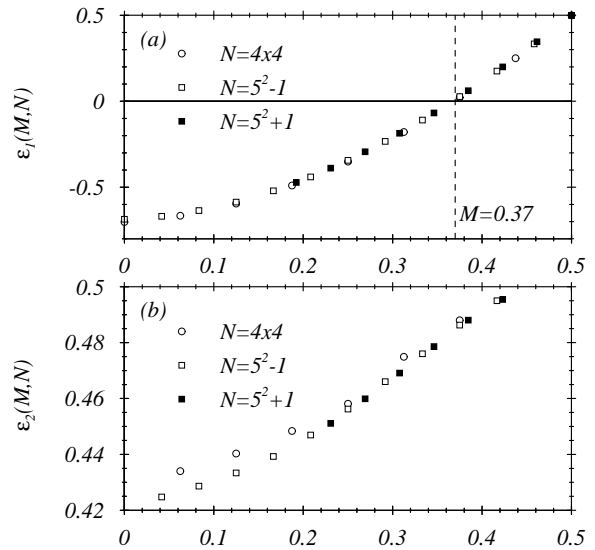


FIG. 1. M -dependence of $\epsilon_{1,2}^M(M)$ for system sizes $N = 4 \times 4$ (square lattice) and $N = 5^2 \pm 1$ (helical boundary conditions)

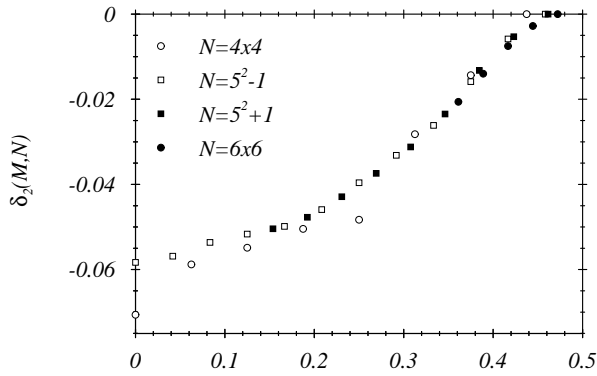


FIG. 2. M - and N -dependence of the second order contribution $\delta_2(M)$

In the collinear antiferromagnetic phase $\alpha > \alpha_0(M)$ perturbation theory in $\beta = 1/\alpha$ to second order yields for the lowest eigenvalue of $H_1 + \alpha H_2$ in the sector with magnetization $M = s/N$:

$$E(s, \mathbf{p}_s, \alpha) = N (2M^2 + \alpha \epsilon_1(M) + \alpha^{-1} \delta_{-1}(M)), \quad \alpha > \alpha_0(M). \quad (2.4)$$

The perturbative results to first order – i.e. the first two terms on the right-hand side of (2.4) – are derived in App. A. Note that this result can be expressed in terms of the ground state energy per site $\epsilon_1(M)$ of the nearest-neighbour model $H = H_1$! The second order contribution $\delta_{-1}(M)$ is computed in App. B.

We would like to stress at this point, that the perturbation expansions (2.1) and (2.4) hold in the thermodynamical limit.

The determination of the coefficients $\epsilon_1(M)$, $\epsilon_2(M)$, $\delta_2(M)$ and $\delta_{-1}(M)$ on finite clusters might be affected by finite-size effects; their magnitude is illustrated in Figs. 1, 2 and 10 and can be reduced by a computation on larger clusters and by a systematic finite-size analysis. The coefficients $\epsilon_1(M)$ and $\epsilon_2(M)$ are related to spin-spin correlators over nearest and next-nearest neighbour sites in the unfrustrated system ($\alpha = 0$). Here, the finite-size effects are small and well under control.

In Fig. 3(a) we show the α -dependence of ground state energies per site $\epsilon(\alpha, M = 1/4)$ as they follow from the perturbation expansions (2.1) and (2.4). The dashed lines represent the contributions to first order, which is fixed by the coefficients

$$\epsilon_1(M = 1/4) = -0.34, \quad \epsilon_2(M = 1/4) = 0.46 \\ \delta_2 = \delta_{-1} = 0.$$

These values can be read off Figs. 1(a), (b). The solid lines include second order contributions. Indeed, second order contributions seem to be relevant only in the antiferromagnetic phase (2.1). They are negligible in the collinear antiferromagnetic phase (2.4). The solid dots represent numerical results for a 4×4 system. Comparison with the perturbative results reveal small finite-size

effects in the antiferromagnetic phase (2.1), however large finite-size effects in the collinear antiferromagnetic phase (2.4).

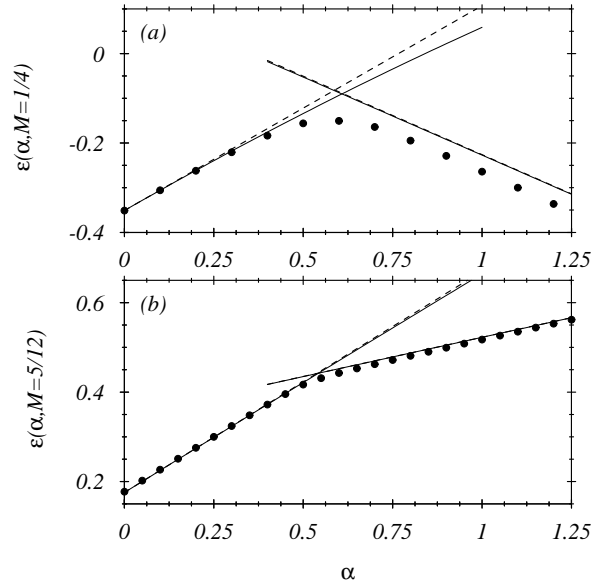


FIG. 3. Comparison of the α -dependence of the ground state energy per site $\epsilon(\alpha, M)$ – $M = 1/4$ (a), $5/12$ (b) – and the perturbation theory results (2.1), (2.4). The numerical data for $M = 1/4$ was taken from a 4×4 system and for $M = 5/12$ from a 6×6 system, both with periodic boundary conditions.

The comparison of the perturbation expansions (2.1) and (2.4) with numerical results for $M = 5/12$ on a larger system with $6 \times 6 = 36$ sites is shown in Fig. 3(b). Note in particular that the deviations in the collinear antiferromagnetic phase are smaller here, owing to the larger system size. In this case, the coefficients turn out to be

$$\epsilon_1(M = 5/12) = 0.17, \quad \epsilon_2(M = 5/12) = 0.49$$

The first order perturbation expansion (2.4) in the collinear antiferromagnetic phase $\alpha > \alpha_0(M)$ predicts the vanishing of the α -dependence for $M_0 \simeq 0.37$, where $\epsilon_1(M_0 \simeq 0.37) = 0$ [cf. Fig. 1(a)].

$$\epsilon(M_0, \alpha) = 2M_0^2 \quad \text{for } \alpha > \alpha_0(M_0). \quad (2.5)$$

Fig. 4(a) shows the M -dependence of $\epsilon(M, \alpha)$ on a 6×6 system for various values of α . All curves with $\alpha > 0.6$ – where the system is in the collinear antiferromagnetic phase – coincide at $M_0 \simeq 0.37$. Data points for $\alpha = 0$ (open circles) – i.e. in the antiferromagnetic phase – do not share this property!

The second derivative of $\epsilon(M, \alpha)$ with respect to M , computed from finite system results with $N = 36$, $\Delta M = 1/N$:

$$\epsilon^{(2)} = \frac{\partial^2 \epsilon}{\partial M^2} = \frac{1}{(\Delta M)^2} \left(\epsilon(M + \Delta M, \alpha) + \epsilon(M - \Delta M, \alpha) - 2\epsilon(M, \alpha) \right) \quad (2.6)$$

is shown in Fig. 4(b).

The data points with $M = 1/2 - 1/N$, $N = 36$ (one spin flipped) have a dip at $\alpha = 1/2$ indicating that the second derivative might vanish here in the thermodynamical limit $N \rightarrow \infty$. Indeed, we see from a Taylor expansion around $M = M_0$:

$$\epsilon(M, \alpha) = \epsilon(M_0, \alpha) + \epsilon^{(1)}(M - M_0) + \frac{1}{2!} \epsilon^{(2)}(M - M_0)^2 + \frac{1}{3!} \epsilon^{(3)}(M - M_0)^3 + \dots, \quad (2.7)$$

$$\epsilon^{(k)} = \left. \frac{\partial^k \epsilon}{\partial M^k} \right|_{M=M_0} \quad (2.8)$$

that the vanishing of the second derivative $\epsilon^{(2)} = 0$ induces a square root singularity in the magnetization curve

$$|M - M_0| \cdot \left| \frac{\epsilon^{(3)}}{2} \right| = |B - B_0|^{1/2}, \quad (2.9)$$

provided that the third derivative $\epsilon^{(3)}$ does not vanish.

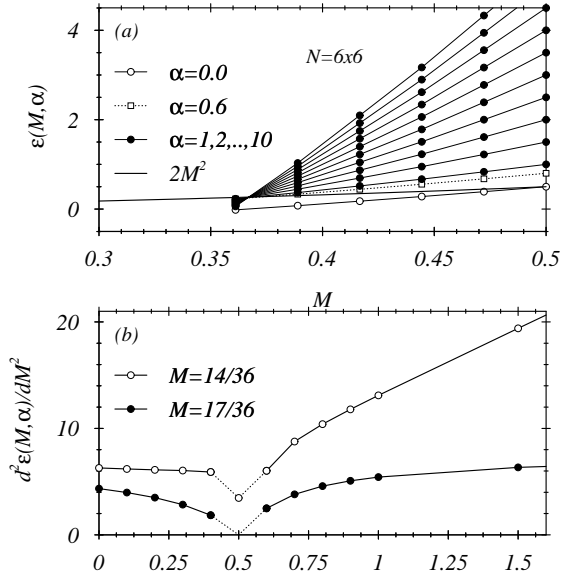


FIG. 4. Ground state energy per site $\epsilon(M, \alpha)$ vs. M – (a) and its second derivative $-\partial^2 \epsilon / \partial M^2$ vs. α – (b).

Under this assumption the numerical results for the magnetization curve at $\alpha = 1/2$ and $M \rightarrow 1/2$ on system sizes $5 \times 5 \pm 1 = 26, 24$, $7 \times 7 \pm 1 = 50, 48$ with helical boundary conditions could be described in Ref. 19 by the square root (2.9).

However, it has been pointed out by Honecker²⁰ in a recent publication, that numerical results on systems of

size 6×6 , 8×8 with periodic boundary conditions indicate that the magnetic fields near saturation

$$B(M = 1/2(1 - n/N), \alpha = 1/2, N) = 4 \quad (2.10)$$

$$\text{for } n = 0, 1, 2, \dots, L, \quad N = L^2$$

are independent of n . This means that the system jumps discontinuously from the magnetization $M = 1/2 \cdot (1 - L/N)$ into the fully magnetized state $M = 1/2$. The size of the jump $\Delta M = L/N$ vanishes in the thermodynamical limit, so one expects a smooth approach to saturation in this limit. Moreover the behaviour (2.10) suggests, that all the derivatives (2.8) near saturation $M_s = 1/2$ vanish, signalling an essential singularity.

Going to a smaller value of M ($M = 14/36 = 0.39$) we find again a dip in the second derivative. However, it is very difficult to locate the dip position with our finite system results.

III. FREE ENERGIES AND MAGNETIZATION CURVES

According to eq. (1.6) the magnetization curves follow from a minimum of the “generalized free energy” per site

$$f(M, \alpha) = \epsilon(M, \alpha) - M \cdot B \quad (3.1)$$

with respect to M at fixed B . The perturbation expansions (2.1) and (2.4) therefore yield for the magnetization curves in the antiferromagnetic and collinear antiferromagnetic phase:

$$B(M, \alpha) = \frac{d\epsilon_1}{dM} + \alpha \frac{d\epsilon_2}{dM} + \alpha^2 \frac{d\delta_2}{dM} \quad (3.2)$$

$$B(M, \alpha) = 4M + \alpha \frac{d\epsilon_1}{dM} + \alpha^{-1} \frac{d\delta_{-1}}{dM}. \quad (3.3)$$

In Fig. 5 we present on the left-hand side the free energies (3.1) – as they follow from (2.1), (2.4) – for $\alpha = 0.5, 0.6, 0.7$.

For $\alpha = 0.5$ [Fig. 5(a)] we are definitely in the antiferromagnetic phase, since the corresponding free energy here (solid line) is below the one in the collinear antiferromagnetic phase (dashed line). In order to demonstrate the quality of the perturbation expansion (2.1) and the numerical data (open circles) on a finite system with $N = 5 \times 5 - 1 = 24$ sites (with helical boundary conditions). Good agreement is found for $M \leq 0.3$. For larger M -values, the numerical data are below the perturbative results.

The corresponding magnetization curves at $\alpha = 0.5$ can be seen on the right-hand side. Again, the first perturbation expansion (3.2) (solid line) follows the numerical results (step function), whereas the second perturbation expansion (3.3) (dashed curve) lies above the numerical results.

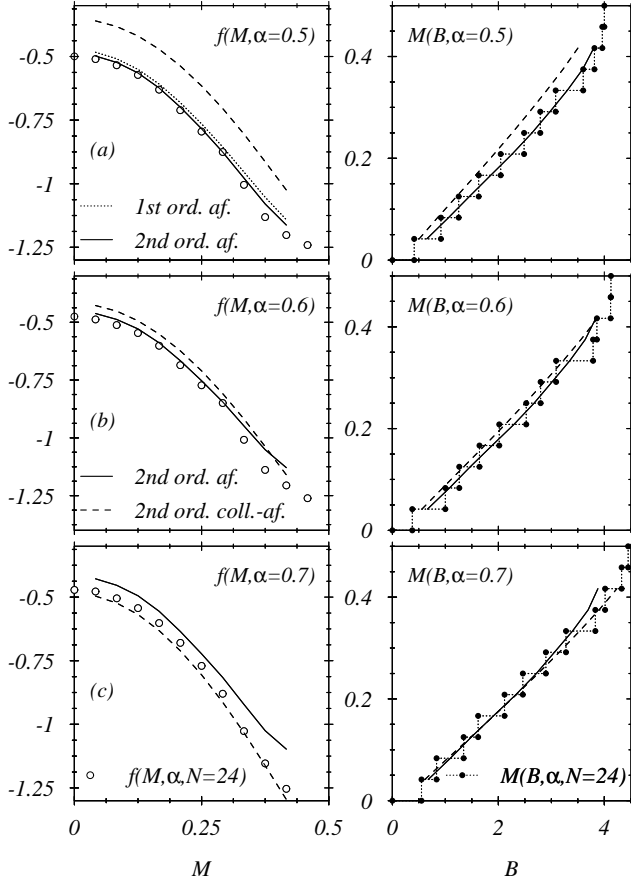


FIG. 5. Free energies and magnetization profiles for $\alpha = 0.5$ (a), 0.6 (b) and 0.7 (c). Solid and dashed curves show the second order perturbation results [cf. (3.2) and (3.3)] in the antiferromagnetic and collinear antiferromagnetic regime, respectively. The circles represent exact diagonalization results on a $N = 5 \times 5 - 1 = 24$ lattice with helical boundary conditions.

For $\alpha = 0.7$ [Fig. 5(c)] we are definitely in the collinear antiferromagnetic phase. The corresponding free energy (dashed line) is now below the one of the antiferromagnetic phase (solid line). The numerical data are close to the dashed line. In the magnetization curve (right-hand side) the perturbation expansions (3.2), (3.3) and the numerical results (step function) coincide for $M < 1/3$.

In between ($0.5 < \alpha < 0.7$) we therefore expect the phase transition. In Fig. 5(b) we show the situation for $\alpha = 0.6$. For $M \leq 1/3$ and $M > 1/3$, the free energies are minimal in the antiferromagnetic and collinear antiferromagnetic phase, respectively. The numerical data (open circles) on the finite system with $N = 24$ sites are lying below the perturbative results. The largest deviations are found in the collinear antiferromagnetic phase ($M > 1/3$) indicating that both perturbation expansions and finite system results become questionable.

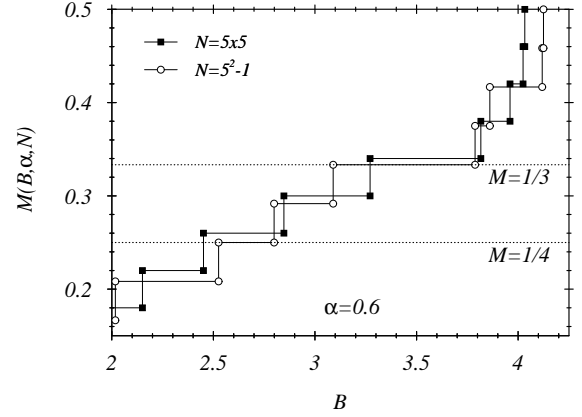


FIG. 6. Behaviour of the magnetization curves of systems with periodic ($N = 5 \times 5$) and helical ($N = 5 \times 5 - 1$) boundary conditions around magnetization $M = 1/4, 1/3$ and frustration $\alpha = 0.6$

For small values of M ($M < 1/3$) the numerical data for the magnetization curve (right-hand side) are well reproduced by the perturbation expansion (3.2) for the antiferromagnetic phase. At $M = 1/3$ a plateau-like structure seems to evolve in the numerical data for $N = 5 \times 5 - 1 = 24$ with helical boundary conditions. Unfortunately, we cannot check whether this structure will survive on larger systems with helical boundary conditions like $N = 7 \times 7 - 1 = 48$. However, the structure seems to appear as well (at $M = 0.34$) on a square lattice $N = 5 \times 5 = 25$ with periodic boundary conditions as is demonstrated in Fig. 6.

IV. DYNAMICAL STRUCTURE FACTORS AND FREQUENCY MOMENT SUM RULES

In this section we will study the impact of the transition from antiferromagnetic to collinear antiferromagnetic order on the dynamical structure factors:

$$S_{jj}(\mathbf{q}, \omega, M, \alpha) = \frac{1}{N} \sum_n \delta(E_n - E_0 - \omega) |\langle n | S_j(\mathbf{q}) | 0 \rangle|^2 \quad (4.1)$$

and their frequency moments:

$$K_n^{(j)}(\mathbf{q}, M, \alpha) = \int_0^\infty d\omega \omega^n S_{jj}(\mathbf{q}, \omega, M, \alpha). \quad (4.2)$$

In particular, we expect signatures in the α -dependence of the structure factors at momenta $\mathbf{q} = (\pi, \pi)$ and $\mathbf{q} = (\pi, 0)$.

In Figs. 7 and 8 we show the α -dependence of the transverse and longitudinal static structure factors on a square lattice with $N = 6 \times 6 = 36$ sites:

$$K_0^{(j)}(\mathbf{q}, M, \alpha, N = 36) \quad \text{for } M = \frac{1}{36} \cdot (13, 14, 15, 16). \quad (4.3)$$

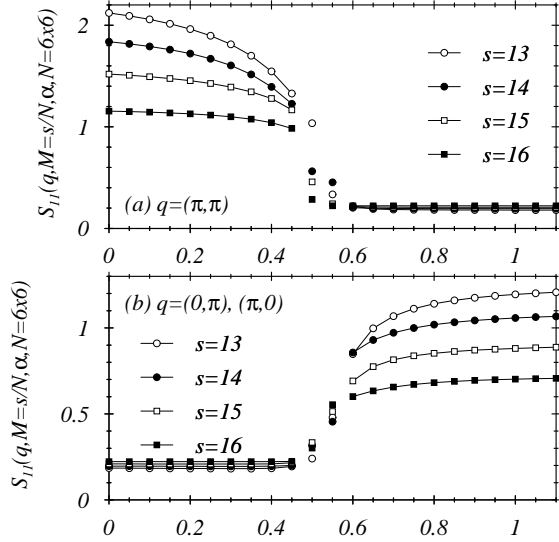


FIG. 7. Zeroth transverse frequency moment (transverse static structure factor) $K_0^{(1)}(\mathbf{q}, M, \alpha) = S_{11}(\mathbf{q}, M, \alpha)$ for system size $N = 6 \times 6$ for different magnetizations and momenta $\mathbf{q} = (\pi, \pi)$ (a) and $\mathbf{q} = (0, \pi), (\pi, 0)$ (b).

The transverse structure factors ($j = 1$) for the momenta $\mathbf{q} = (\pi, \pi)$ [Fig. 7(a)] and $\mathbf{q} = (\pi, 0), (0, \pi)$ [Fig. 7(b)] reveal a striking similarity in their α -dependence: All curves for $\mathbf{q} = (\pi, \pi)$ and $\mathbf{q} = (\pi, 0), (0, \pi)$ show a sensitive change in their M - and α -dependence when entering the regimes $\alpha > 0.6$ and $\alpha < 0.5$, respectively.

In particular we see in our data, that

$$S_{11}(\mathbf{q} = (\pi, \pi), M, \alpha) \simeq M/2 \quad \text{for } \alpha > 0.6. \quad (4.4)$$

This behaviour is a consequence of the ground state wave function (A2).

The longitudinal structure factor [(4.3) for $j = 3$] at the momenta $\mathbf{q} = (\pi, \pi)$ [Fig. 8(a)] and $\mathbf{q} = (\pi, 0), (0, \pi)$ [Fig. 8(b)] look similar in the small- α regime ($\alpha < 0.5$): One observes a constant behaviour with α and a monotonic decrease with M . For large values α , the longitudinal structure factors behave quite differently: For $\mathbf{q} = (\pi, \pi)$ the curves with $M = s/N$, s even and s odd approach different limiting values, respectively. This feature is not visible for $\mathbf{q} = (\pi, 0), (0, \pi)$.

Numerical data for the static structure factor on a 6×6 system with periodic boundary conditions have been presented in.¹⁵ At fixed magnetization $M = 1/4$ – where the authors see a plateau in the magnetization curve – the data points for the longitudinal structure factor at $\mathbf{q} = (\pi, \pi)$ and $\mathbf{q} = (\pi, 0)$ show a broad maximum in the regime $0.55 \leq \alpha \leq 0.67$, which is also visible in our results for larger M values [cf. Figs. 8(a), (b) in the interval $0.5 < \alpha < 0.6$].

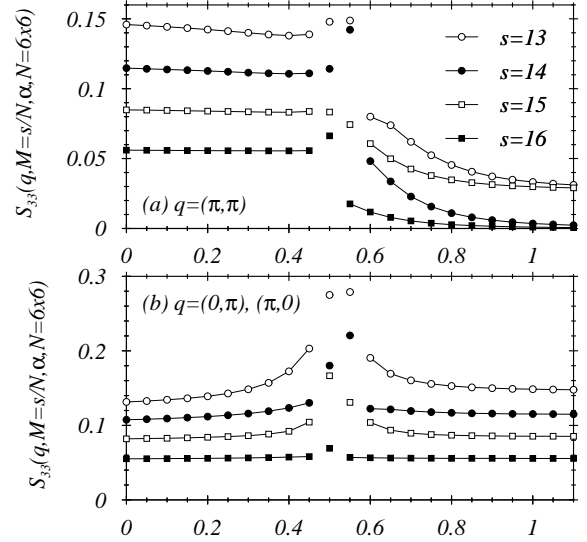


FIG. 8. Zeroth longitudinal frequency moment (longitudinal static structure factor) $K_0^{(3)}(\mathbf{q}, M, \alpha) = S_{33}(\mathbf{q}, M, \alpha)$ for system size $N = 6 \times 6$ for different magnetizations and momenta $\mathbf{q} = (\pi, \pi)$ (a) and $\mathbf{q} = (0, \pi), (\pi, 0)$ (b).

Let us next turn to the first frequency moment. As was pointed out by Hohenberg and Brinkman²¹ and Müller²² it can be expressed in terms of ground state expectation values for two-fold commutators:

$$\begin{aligned} K_1^{(j)}(\mathbf{q}, M, \alpha) &= \frac{1}{N} \sum_n (E_n - E_0 - B(S_{3n} - S_{30})) \\ &\quad \times |\langle n | S_j(\mathbf{q}) | 0 \rangle|^2 \\ &= \frac{1}{N} \langle 0 | S_j^+(\mathbf{q}) H S_j(\mathbf{q}) - H S_j^+(\mathbf{q}) S_j(\mathbf{q}) | 0 \rangle \\ &= \frac{1}{2N} \langle 0 | [[S_j^+(\mathbf{q}), H], S_j(\mathbf{q})] | 0 \rangle. \end{aligned} \quad (4.5)$$

S_{30} and S_{3n} are the 3-component of the total spin in the ground state $|0\rangle$ and the excited states $|n\rangle$, respectively. The calculation of the commutators yields:

$$\begin{aligned} K_1^{(j)}(\mathbf{q}, M, \alpha) &= -(1 - \cos q_1) C_j(\hat{1}) - (1 - \cos q_2) C_j(\hat{2}) \\ &\quad - \alpha (1 - \cos(q_1 + q_2)) C_j(\hat{1} + \hat{2}) \\ &\quad - \alpha (1 - \cos(q_1 - q_2)) C_j(\hat{1} - \hat{2}) \\ &\quad - \frac{1}{2} M_j B(M, \alpha), \end{aligned} \quad (4.6)$$

where

$$\begin{aligned} C_j(\hat{\nu}) &= \frac{1}{N} \sum_{\mathbf{x}} (\langle 0 | \mathbf{S}(\mathbf{x}) \mathbf{S}(\mathbf{x} + \hat{\nu}) | 0 \rangle \\ &\quad - \langle 0 | S_j(\mathbf{x}) S_j(\mathbf{x} + \hat{\nu}) | 0 \rangle) \end{aligned} \quad (4.7)$$

for $j = 1, 2, 3$, $\hat{\nu} = \hat{1}, \hat{2}, \hat{1} + \hat{2}, \hat{1} - \hat{2}$ and

$$\begin{aligned} M_j &= M \quad \text{for } j = 1, 2, \\ M_j &= 0 \quad \text{for } j = 3. \end{aligned}$$

It should be noted that the dependence on the momentum transfer $\mathbf{q} = (q_1, q_2)$ is completely given by the Fourier factors on the right-hand side of (4.6). The physical meaning of the first frequency moment can be seen from the definitions (4.1) and (4.2).

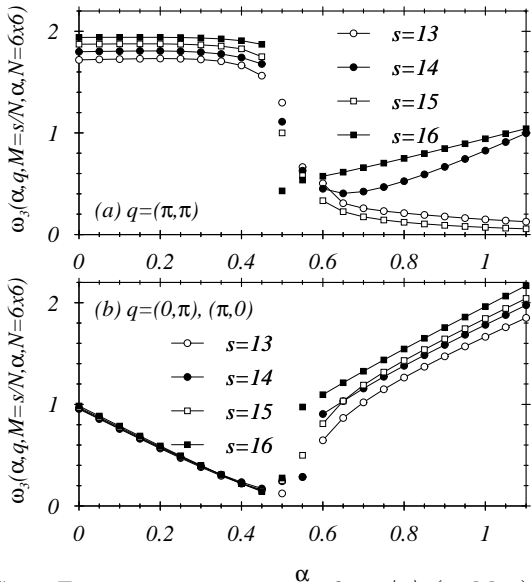


FIG. 9. Frequency expectation values $\langle \omega \rangle_3(\mathbf{q}, M, \alpha)$ for a $N = 6 \times 6$ spin system for different magnetizations and $\mathbf{q} = (\pi, \pi)$ (a) and $\mathbf{q} = (0, \pi), (\pi, 0)$ (b).

The ratio

$$\langle \omega_j \rangle(\mathbf{q}, M, \alpha) = \frac{K_1^{(j)}(\mathbf{q}, M, \alpha)}{K_0^{(j)}(\mathbf{q}, M, \alpha)}, \quad j = 1, 3 \quad (4.8)$$

yields the average excitation energy in the spectrum of states which can be reached from the ground state $|0\rangle = |\mathbf{p}_s, M_s\rangle$ by means of the operator $S_j(\mathbf{q})$ $j = 1, 2, 3$. This ratio is shown for the longitudinal case $j = 3$ and magnetizations $M = 1/36 \cdot (13, 14, 15, 16)$ on a 6×6 system in Fig. 9.

At momentum $\mathbf{q} = (\pi, \pi)$ [Fig. 9(a)], we observe a sharp drop in the width of the excitation spectrum at $\alpha \approx 0.5$, i.e. close to the phase boundary.

At $\mathbf{q} = (\pi, 0), (0, \pi)$ [Fig. 9(b)] the longitudinal structure factors for all M -values follow the same straight line, which ends at a minimum at $\alpha = 0.5$.

V. CONCLUSIONS AND DISCUSSION

The magnetization process in the two-dimensional $J_1 - J_2$ model is well described in the antiferromagnetic phase ($\alpha < 0.5$) by a perturbation expansion around $\alpha = 0$ and in the collinear antiferromagnetic phase ($\alpha > 0.7$) by a perturbation expansion around $\alpha^{-1} = 0$. In these regimes, the magnetization curves are smooth, monotonically increasing and convex. The change in the magnetic

order can be seen in the α -dependence of the transverse and longitudinal structure factors at momenta $\mathbf{q} = (\pi, \pi)$ and $\mathbf{q} = (\pi, 0), (0, \pi)$, respectively.

Using frequency moment sum rules we have also studied the variation of the average excitation energy $\langle \omega \rangle$ (4.8) with α . Approaching the transition region from antiferromagnetic to collinear antiferromagnetic order, the spectral weight is more and more concentrated around low frequencies.

Between the antiferromagnetic and collinear antiferromagnetic phase – i.e. for $0.5 < \alpha < 0.7$ – a phase of transverse disorder has been suggested.¹⁵

This regime is not accessible with the perturbative methods developed in this paper; nonperturbative effects – like plateaus – are expected here.

To study these, we have to rely on numerical results on finite clusters. The results available so far reveal a strong dependence on the size of the clusters and the boundary conditions. For the moment we meet the following situation:

(A) At $\alpha = 1/2$ the approach to saturation ($M_s = 1/2$) is no longer linear but appears to develop a singularity. The type of the singularity is not yet clear:

On one hand, numerical data on square lattices $6 \times 6 = 36$, $8 \times 8 = 64$ with periodic boundary conditions reveal the peculiar property (2.10) for the magnetic fields near saturation. If we assume in the thermodynamic limit a series expansion [cf. (2.7)] of the energies per site $\epsilon(M, \alpha)$ at the saturation point $M_s = 1/2$, infinitely many derivatives [cf. (2.8)] would vanish, indicating an essential singularity.

On the other hand, numerical results [Ref. 19] on finite lattices $5 \times 5 \pm 1 = 26, 24$, $7 \times 7 \pm 1 = 50, 48$ with helical boundary conditions do not share the property (2.10) for the magnetic fields near saturation $M \rightarrow 1/2$, $\alpha = 1/2$. It was suggested in Ref. 19 that the magnetization curve develops a square root singularity, which follows if the second derivative $\epsilon^{(2)}(M, \alpha = 1/2)$ in (2.7) vanishes for $M \rightarrow 1/2$, but not the higher ones $\epsilon^{(k)}(M, \alpha = 1/2)$ $k = 3, 4, \dots$

(B) At $\alpha = 0.6$ strong evidence for a plateau at $M = 1/4$ has been reported by Honecker et al.^{15,20} who performed a finite-size analysis of exact diagonalization results on 3 clusters 4×4 , 4×6 and 6×6 with periodic boundary conditions. They do not find any signature for a plateau at $M = 1/3$. In our results obtained from a $N = 5 \times 5 - 1 = 24$ system with helical boundary conditions we do not find a plateau at $M = 1/4$; but there are indications for a plateau-like structure at $M = 1/3$. We are aware of the fact, that this discrepancy might come from special finite-size effects due to the helical boundary conditions, which only disappear for much larger systems (e.g. $N = 7 \times 7 - 1 = 48, \dots$). However, these are not yet accessible.

In order to test the dependence on the boundary conditions we have compared the magnetization curves for $N = 5 \times 5 - 1 = 24$ with helical boundary conditions and for $N = 5 \times 5 = 25$ with periodic boundary conditions.

The results (Fig. 6) look similar. This would mean that the plateau structures in the magnetization curve has a sensitive dependence on the system size $N = L \times L$; in particular results for L even and L odd might be quite different. Therefore, the precise determination of the positions and widths of the plateaus in the frustrated Heisenberg model is indeed a very delicate problem.

A better theoretical understanding of the magnetic order and of the mechanisms which create the plateaus is really needed.

ACKNOWLEDGMENTS

We would like to thank M. Karbach for discussion and a critical reading of the manuscript.

APPENDIX A: THE STRONG FRUSTRATION LIMIT

As was pointed out in Sec. I [cf. (1.10)], the diagonal couplings build up two independent nearest-neighbour Hamiltonians on the even and odd sublattice, respectively.

We start with the eigenvalue equations for these sublattices

$$\left. \begin{array}{l} H_1^{(\pm)} \\ \mathbf{S}^2 \\ S_3 \end{array} \right\} \Psi^{(\pm)}(\sigma, \mathbf{p}_\sigma) = \left. \begin{array}{l} E(\sigma, \mathbf{p}_\sigma) \\ \sigma(\sigma + 1) \\ \sigma \end{array} \right\} \Psi^{(\pm)}(\sigma, \mathbf{p}_\sigma). \quad (\text{A1})$$

In particular we are interested in the ground state with definite (squared) total spin and total magnetization $M = \sigma/(N/2)$. In the thermodynamical limit $N/2 \rightarrow \infty$ the ground state momenta \mathbf{p}_σ follow Marshall's sign rule¹³. If $N/4 + \sigma$ is even, the ground state momentum turns out to be $\mathbf{p}_\sigma = (0, 0)$; if $N/4 + \sigma$ is odd, one obtains $\mathbf{p}_\sigma = (\pi, \pi)$. The lowest eigenstates of the Hamiltonian $H_2 = H_1^{(+)} + H_1^{(-)}$ with even total spin and zero total momentum $\mathbf{p} = (0, 0)$ can be constructed as a product of states of the lowest eigenstates (A1) of the subsystems:

$$\begin{aligned} \Psi(s, \mathbf{p}_s = (0, 0), N) &= \Psi^{(+)}(s/2, \mathbf{p}_{s/2}, N/2) \\ &\times \Psi^{(-)}(s/2, \mathbf{p}_{s/2}, N/2). \end{aligned} \quad (\text{A2})$$

The two subsystems defined on the even and odd sites can be transformed into each other via a translation of one lattice spacing. We can therefore impose the following identification on the wave functions with identical quantum numbers in (A2)

$$\Psi^{(-)}(\sigma, \mathbf{p}_\sigma, N/2) = T_1 \Psi^{(+)}(\sigma, \mathbf{p}_\sigma, N/2), \quad \sigma = 1/2. \quad (\text{A3})$$

(A3) guarantees that the product states (A2) are invariant under both ($\nu = 1, 2$) translation operators:

$$T_\nu \Psi(s, \mathbf{p}_s = (0, 0), N) = \Psi(s, \mathbf{p}_s = (0, 0), N), \quad (\text{A4})$$

i.e. they are momentum zero eigenstates. For the proof of this statement one has to realize that the eigenstates on the subsystems behave as follows under translations:

$$\begin{aligned} T_1 T_2 \Psi^{(\pm)}(\sigma, \mathbf{p}, N/2) &= e^{ip_1} \cdot \Psi^{(\pm)}(\sigma, \mathbf{p}, N/2) \\ T_1 T_2^{-1} \Psi^{(\pm)}(\sigma, \mathbf{p}, N/2) &= e^{ip_2} \cdot \Psi^{(\pm)}(\sigma, \mathbf{p}, N/2) \\ T_1^2 \Psi^{(\pm)}(\sigma, \mathbf{p}, N/2) &= e^{i(p_1+p_2)} \cdot \Psi^{(\pm)}(\sigma, \mathbf{p}, N/2) \end{aligned} \quad (\text{A5})$$

It should be noted that the product states (A2) where the total spin s is distributed to equal parts on the two sublattices indeed yields the ground state with energy

$$E(s, \mathbf{p}_s = (0, 0), N) = 2E(s/2, \mathbf{p}_{s/2}, N/2). \quad (\text{A6})$$

Any other distribution, e.g. with a total spin $s/2 + \Delta s$ on the even and $s/2 - \Delta s$ on the odd lattice will lead to an eigenstate with higher energy. This is a consequence of the fact that the lowest energy is monotonically increasing and a convex function of the magnetization $M = s/N$.

The construction of eigenstates of $H_1^{(+)} + H_1^{(-)}$ with odd total spin s and total momentum $\mathbf{p}_s = (\pi, 0), (0, \pi)$ is more involved. In this case an equal distribution of the total spin on the two sublattices is impossible since the sublattice spin σ has to be integer. The state with lowest energy is found with the ansatz:

$$\begin{aligned} \Psi(s, \mathbf{p}_s = (\pi, 0), N) &= \\ \frac{1}{\sqrt{2}} &\left(\Psi^{(+)}(\sigma, \mathbf{p}_\sigma, N/2) \Psi^{(-)}(\sigma - 1, \mathbf{p}_{\sigma-1}, N/2) \right. \\ &\left. - \Psi^{(+)}(\sigma - 1, \mathbf{p}_{\sigma-1}, N/2) \Psi^{(-)}(\sigma, \mathbf{p}_\sigma, N/2) \right) \end{aligned} \quad (\text{A7})$$

where

$$\sigma = \frac{s+1}{2}. \quad (\text{A8})$$

Imposing the identification (A3) on the ground states with equal quantum numbers, one finds the following transformation properties of the states (A7):

$$\begin{aligned} T_1 \Psi(s, \mathbf{p}_s = (\pi, 0), N) &= -\Psi(s, \mathbf{p}_s = (\pi, 0), N) \\ T_2 \Psi(s, \mathbf{p}_s = (\pi, 0), N) &= \Psi(s, \mathbf{p}_s = (\pi, 0), N) \end{aligned} \quad (\text{A9})$$

which means that the ground state momentum is $\mathbf{p}_s = (\pi, 0)$. The degenerate ground state with momentum $\mathbf{p}_s = (0, \pi)$ is obtained if we substitute the translation operator T_1 by T_2 in (A3).

In the strong coupling limit $\alpha \rightarrow \infty$ ($\beta = 1/\alpha \rightarrow 0$), the nearest-neighbour operator H_1 in (1.1) acts as a perturbation operator and we therefore have to compare in first order the expectation values of H_1 between the ground states (A2) and (A7), respectively:

$$\begin{aligned}
& \langle \Psi(s, \mathbf{p}_s = (0, 0), N) | H_1 | \Psi(s, \mathbf{p}_s = (0, 0), N) \rangle \\
&= \sum_{\mathbf{x} \in (+)} \langle \Psi^{(+)}(\sigma) | S_3(\mathbf{x}) | \Psi^{(+)}(\sigma) \rangle \\
& \quad \times \sum_{\nu} \langle \Psi^{(-)}(\sigma) | T_{\nu} S_3(\mathbf{x}) T_{\nu}^{-1} | \Psi^{(-)}(\sigma) \rangle. \quad (\text{A10})
\end{aligned}$$

Here we have used the fact that the nearest-neighbour couplings in H_1 connect the spin operator $\mathbf{S}(\mathbf{x})$ on the even sub-lattice with the spin operators $\mathbf{S}(\mathbf{y} = \mathbf{x} + \nu) = T_{\nu} \mathbf{S}(x) T_{\nu}^{-1}$ on the odd sub-lattice.

According to (A3) and (A5) the application of the translation operator T_{ν} yields:

$$\begin{aligned}
& \sum_{\nu} \langle \Psi^{(-)}(\sigma) | T_{\nu} S_3(\mathbf{x}) T_{\nu}^{-1} | \Psi^{(+)} \rangle \\
&= 4 \cdot \langle \Psi^{(+)}(\sigma) | S_3(\mathbf{x}) | \Psi^{(+)}(\sigma) \rangle \quad (\text{A11}) \\
&= 4 \cdot \frac{1}{N/2} \cdot \sigma, \quad \sigma = s/2, \\
&= 4M.
\end{aligned}$$

We end up with the following expression for the ground state energies in the antiferromagnetic collinear phase $\alpha > \alpha_0(M)$ in the first order approximation:

$$\begin{aligned}
E(s, \mathbf{p}_s = (0, 0), \alpha, N) &= \alpha \left(2E(s/2, \mathbf{p}_{s/2} = (0, 0), N/2) \right. \\
& \quad \left. + \frac{1}{\alpha} 2M^2 \cdot N \right) \quad (\text{A12})
\end{aligned}$$

We compute in the same manner the expectation values of H_1 between the ground state (A7) for s odd, $\sigma = s/2 + 1$ even ($\mathbf{p}_s = (0, \pi)$):

$$\begin{aligned}
E(s, \mathbf{p}_s = (0, \pi), \alpha, N) &= \alpha \left(E(\sigma, \mathbf{p}_{\sigma} = (0, 0), N/2) \right. \\
& \quad \left. + E(\sigma - 1, \mathbf{p}_{\sigma} = (\pi, \pi), N/2) \right. \\
& \quad \left. + \frac{1}{\alpha} 2M^2 N \right). \quad (\text{A13})
\end{aligned}$$

APPENDIX B: SECOND ORDER PERTURBATION THEORY IN THE STRONG FRUSTRATION LIMIT

The evolution of the energy eigenvalues and transition matrix elements of a Hamiltonian

$$H_2 + \beta H_1 \quad (\text{B1})$$

depending on some parameter β is described by a closed system of differential equations²³. In particular one finds for the second derivative of the ground state energy:

$$\frac{d^2 E_0}{d\beta^2} = -2 \sum_n \frac{|T_{n0}|^2}{E_n - E_0} \quad (\text{B2})$$

where

$$T_{n0} = \langle n | H_1 | 0 \rangle. \quad (\text{B3})$$

$|0\rangle$ and $|n\rangle$ denote the ground state and the excited states of (B1) with energy eigenvalues E_0 and E_n , respectively.

We are now going to evaluate (B2) in the strong frustration limit $\beta = 1/\alpha \rightarrow \infty$. The ground state of H_2 in the sector with total spin s ($s/2$ even) is given in (A2). In the following we will consider those contributions to the transition amplitudes, which arise from the excited states:

$$\begin{aligned}
\Psi^*(s, \mathbf{p}_s = (0, 0), N) &= \\
& \frac{1}{\sqrt{2}} \left(\Psi^{(+)}(\sigma + 1, \mathbf{p}, N/2) \Psi^{(-)}(\sigma - 1, -\mathbf{p}, N/2) \right. \\
& \quad \left. + \Psi^{(+)}(\sigma - 1, -\mathbf{p}, N/2) \Psi^{(-)}(\sigma + 1, \mathbf{p}, N/2) \right) \quad (\text{B4})
\end{aligned}$$

with energy $E^{(+)}(\sigma + 1, \mathbf{p}, N/2) + E^{(-)}(\sigma - 1, \mathbf{p}, N/2)$ and $\sigma = s/2$. $E^{(\pm)}(\sigma', \mathbf{p}, N/2)$ are the lowest energies on the subsystems for a given spin σ' and momentum \mathbf{p} . The momenta \mathbf{p} and $-\mathbf{p}$ on the subsystems have to add up to zero in order to produce a translationally invariant (momentum $\mathbf{p}_s = \mathbf{0}$) state on the whole lattice. Similarly the sublattice spins $\sigma + 1$ and $\sigma - 1$ add up to the total spin s of the whole system. Any other distribution of the total spin s on the sublattices will increase the total energy in comparison with $E^{(+)}(\sigma + 1, \mathbf{p}, N/2) + E^{(-)}(\sigma - 1, \mathbf{p}, N/2)$.

The computation of the transition matrix elements yields:

$$\begin{aligned}
& \langle \Psi_{\sigma+1, \mathbf{p}}^{(+)} \Psi_{\sigma-1, -\mathbf{p}}^{(-)} | H_1 | \Psi_{\sigma, \mathbf{p}_{\sigma}=(0,0)}^{(+)} \Psi_{\sigma, \mathbf{p}_{\sigma}=(0,0)}^{(-)} \rangle \\
&= \sum_{\mathbf{x} \in (+)} \langle \Psi_{\sigma+1, \mathbf{p}}^{(+)} | S_+(x) | \Psi_{\sigma, \mathbf{p}_{\sigma}=(0,0)}^{(+)} \rangle \\
& \quad \times \sum_{\nu} \langle \Psi_{\sigma-1, -\mathbf{p}}^{(-)} | T_{\nu} S_-(\mathbf{x}) T_{\nu}^{+} | \Psi_{\sigma, \mathbf{p}_{\sigma}=(0,0)}^{(-)} \rangle \\
&= \frac{N}{2} \cdot \left(1 + e^{ip_1} + e^{ip_2} + e^{i(p_1+p_2)} \right) \\
& \quad \times \langle \Psi_{\sigma+1, \mathbf{p}}^{(+)} | S_+(\mathbf{x} = \mathbf{0}) | \Psi_{\sigma, \mathbf{p}=(0,0)}^{(+)} \rangle \\
& \quad \times \langle \Psi_{\sigma-1, -\mathbf{p}}^{(-)} | S_-(\mathbf{x} = \mathbf{0}) | \Psi_{\sigma, \mathbf{p}=(0,0)}^{(-)} \rangle. \quad (\text{B5})
\end{aligned}$$

Here we have used the transformation properties (A5) of the sublattice eigenstates $\Psi^{(\pm)}(\sigma \pm 1, \mathbf{p})$ under the translation operators T_{ν} .

A similar expression for the transition matrix elements to the second component in the excited state (B4), is obtained by the substitution $\mathbf{p} \rightarrow -\mathbf{p}$ in the prefactor on the right-hand side of (B5).

Combining both results, we obtain for the transition probabilities to the excited states (B4):

$$\begin{aligned}
|T_{n0}|^2 &= |\langle \Psi_{s,\mathbf{p}_s}^* | H_1 | \Psi_{s,\mathbf{p}_s}^* \rangle|^2 \quad ; \quad \mathbf{p}_s = (0, 0) \\
&= 2 \left(\frac{N}{2} \right)^2 \cdot (1 + \cos p_1)^2 (1 + \cos p_2)^2 \\
&\quad \times |\langle \Psi_{\sigma+1,\mathbf{p}}^{(+)} | S_+(0) | \Psi_{\sigma,\mathbf{p}\sigma=(0,0)}^{(+)} \rangle|^2 \\
&\quad \times |\langle \Psi_{\sigma-1,-\mathbf{p}}^{(+)} | S_-(0) | \Psi_{\sigma,\mathbf{p}\sigma=(0,0)}^{(+)} \rangle|^2. \quad (\text{B6})
\end{aligned}$$

For the evaluation of the second order term (B2) in the perturbation expansion of (B1) around $\beta = 1/\alpha = 0$ we also need the energy differences

$$\begin{aligned}
E_n - E_0 &= E_{n_1}(\mathbf{p}, \sigma + 1, N/2) + E_{n_2}(-\mathbf{p}, \sigma - 1, N/2) \\
&\quad - 2E_0(\mathbf{p}_0 = \mathbf{0}, \sigma, N/2). \quad (\text{B7})
\end{aligned}$$

We have computed the energy differences

$$\begin{aligned}
E_{n_l}(\mathbf{p}, \sigma \pm 1, N/2) - E_0(\mathbf{p}_0 = \mathbf{0}, \sigma, N/2), \\
\sigma = s/2, \quad l = 1, 2
\end{aligned}$$

on the \pm -subsystems as well as the transition probabilities

$$|\langle \Psi_{n_l, \sigma \pm 1, \pm \mathbf{p}}^{(+)*} | S_{\pm}(0) | \Psi_{\sigma, \mathbf{p}\sigma=\mathbf{0}} \rangle|^2 \quad (\text{B8})$$

by means of the recursion method¹⁷. The resulting coefficient $\delta_{-1}(M)$, which appears in the expansion (2.4):

$$\delta_{-1}(M) = -\frac{1}{N} \sum_{n_1, n_2} \sum_{p_1, p_2} \frac{|T_{n0}|^2}{E_n - E_0} \quad (\text{B9})$$

is shown in Fig. 10.

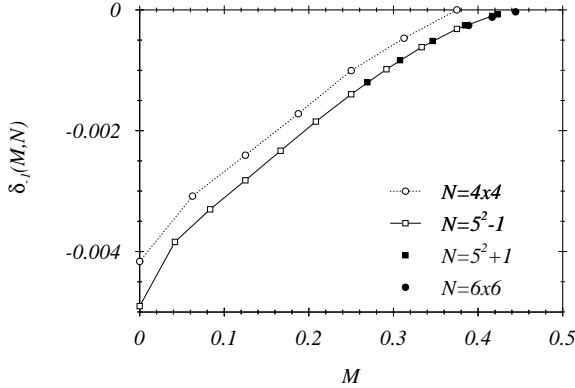


FIG. 10. M - and N -dependence of the second order contribution $\delta_{-1}(M)$

- ² A. Fledderjohann, C. Gerhardt, M. Karbach, K.-H. Mütter, and R. Wiessner, Phys. Rev. B **59**, 991 (1999)
- ³ E. Lieb, T. Schultz, and D. Mattis, Annals of Phys. **16**, 407 (1961)
- ⁴ H. Nojiri, Y. Tabunaga, and M. Motokawa, J. de Physique **49**, C8 1459 (1988)
- ⁵ A. Honecker, M. Kaulke, and K. D. Schotte, Eur. Phys. J. B **15**, 423 (2000)
- ⁶ W. Shiramura et al., J. Phys. Soc. Jpn. **67**, 1548 (1998)
- ⁷ A. K. Kolezhuk, Phys. Rev. B **59**, 4181 (1999)
- ⁸ K. Onizuka, H. Kageyama et al., J. Phys. Soc. Jpn. **69**, 1016 (2000)
- ⁹ B. S. Shastry, B. Sutherland, Physica **108B**, 1308 (1981)
- ¹⁰ S. Miyahara, K. Ueda, Phys. Rev. Lett. **82**, 3701 (1999)
- ¹¹ E. Müller-Hartmann, R. P. Singh, C. Knetter, and G. Uhrig, Phys. Rev. Lett. **84**, 1808 (2000)
- ¹² T. Momoi, K. Totsuka, Phys. Rev. B **62**, 15067 (2000); Y. Fukumoto, A. Oguchi, J. Phys. Soc. Jpn. **69**, 1286 (2000); Y. Fukumoto, J. Phys. Soc. Jpn. **70**, 1397 (2001)
- ¹³ W. Marshall, Proc. Roy. Soc. (London) A **232**, 48 (1955)
- ¹⁴ H. J. Schulz, T. A. L. Ziman, Europhys. Lett. **18**, 355 (1992)
- ¹⁵ M. E. Zhitomirsky, A. Honecker, and O. A. Petrenko, Phys. Rev. Lett. **85**, 3269 (2000)
- ¹⁶ Yu. E. Lozovik, O. I. Notych, Solid St. Commun. **85**, 873 (1993)
- ¹⁷ A. Fledderjohann, M. Karbach, K.-H. Mütter, and P. Wielath, J. Phys. C **7**, 8993 (1995); A. Fledderjohann, K.-H. Mütter, M.-S. Yang, and M. Karbach, Phys. Rev. B **57**, 956 (1998)
- ¹⁸ K. Fabricius, U. Löw, and K.-H. Mütter, Phys. Rev. B **44**, 9981 (1991)
- ¹⁹ M.-S. Yang, K.-H. Mütter, Z. Phys. B **104**, 117 (1997)
- ²⁰ A. Honecker, preprint (2000)
- ²¹ P. C. Hohenberg, W. F. Brinkman, Phys. Rev. B **10**, 128 (1974)
- ²² G. Müller, Phys. Rev. B **26**, 1311 (1982)
- ²³ A. Fledderjohann, K.-H. Mütter, and M. Karbach, Europ. Phys. J. B **5**, 487 (1998)

¹ M. Oshikawa, M. Yamanaka, and I. Affleck, Phys. Rev. Lett. **78**, 1984 (1997)